metals

MDPI

Article

Fatigue Behavior of Cu-Zr Metallic Glasses under Cyclic Loading

Nikolai V. Priezjev [1,2]

[1] Department of Civil and Environmental Engineering, Howard University, Washington, DC 20059, USA; nikolai.priezjev@howard.edu
[2] Department of Mechanical and Materials Engineering, Wright State University, Dayton, OH 45435, USA

Abstract: The effect of oscillatory shear deformation on the fatigue life, yielding transition, and flow localization in metallic glasses is investigated using molecular dynamics simulations. We study a well-annealed Cu-Zr amorphous alloy subjected to periodic shear at room temperature. We find that upon loading for hundreds of cycles at strain amplitudes just below a critical value, the potential energy at zero strain remains nearly constant and plastic events are highly localized. By contrast, at strain amplitudes above the critical point, the plastic deformation is gradually accumulated upon continued loading until the yielding transition and the formation of a shear band across the entire system. Interestingly, when the strain amplitude approaches the critical value from above, the number of cycles to failure increases as a power-law function, which is consistent with the previous results on binary Lennard-Jones glasses.

Keywords: yielding transition; metallic glasses; fatigue life; periodic deformation; molecular dynamics simulations

Citation: Priezjev, N.V. Fatigue Behavior of Cu-Zr Metallic Glasses under Cyclic Loading. *Metals* **2023**, *13*, 1606. https://doi.org/10.3390/met13091606

Academic Editor: Yong Zhang and Yonggang Yao

Received: 17 August 2023
Revised: 12 September 2023
Accepted: 15 September 2023
Published: 17 September 2023

1. Introduction

Understanding structure–property–function relationships in bulk metallic glasses, which exhibit exceptionally high strength and large elastic limit, is important for various engineering applications [1,2]. Under cyclic loading at sufficiently large stress or strain amplitudes, such amorphous alloys ultimately fail through the formation of nanoscale shear bands and propagation of microscale cracks [3,4]. Fatigue tests in experiments typically involve 10^7 stress-controlled loading cycles until fracture is detected, depending on chemical composition, cycling frequency, sample size, and loading condition [5]. On the microscopic level, an elementary plastic deformation process in disordered alloys involves a swift collective rearrangement of a few tens of atoms or a shear transformation [6,7]. Using a mean field elastoplastic model with a distribution of local yield barriers, it was recently demonstrated that the fatigue life of athermal amorphous solids follows a power-law divergence when the yielding point is approached from above [8]. Furthermore, within two models of elastoplastic rheology, it was found that fatigue in amorphous materials proceeds via slow accumulation of low levels of damage and it is followed by a sudden failure and shear band formation after a number of cycles that, in turn, depend on the degree of annealing prior to loading, strain amplitude, and working temperature [9]. Despite recent advances, however, the exact mechanism of fatigue failure in metallic glasses and an accurate prediction of the fatigue life remain not fully understood.

In the last few years, the effect of cyclic loading on rejuvenation, relaxation, and yielding phenomena in amorphous alloys was extensively studied using particle-based simulations [10–42]. In particular, it was found that after a number of transient cycles, athermal glasses undergo strain-induced reversible deformation where atomic trajectories become identical during one or more periods [11,13]. Whereas poorly annealed glasses tend to relax when subjected to small-amplitude cyclic shear [12,22,24,27,29], well-annealed amorphous alloys can be rejuvenated during a number of cycles before yielding at strain amplitudes above a critical point [33,35,42]. The yielding transition in periodically deformed

glasses typically proceeds through the formation of shear bands that are initiated either at open boundaries [14,15,26,36,39] or in the bulk of the computational domain in case of periodic boundary conditions [20,21,23,24,28,33,37,40,42]. In the vicinity of a critical strain amplitude, the number of cycles until the yielding transition depends on temperature [33], preparation history [20,28,37,40], strain amplitude [15,20,21,33], deformation protocol [30], and loading frequency [15]. Notably, it was recently demonstrated that fatigue failure in well-annealed binary Lennard-Jones (LJ) glasses occurs after a number of shear cycles that increases as a power-law function when the loading amplitude approaches a critical value [42]. In spite of significant progress, however, the role of loading protocol, processing history, and interaction potentials on the fatigue life and yielding transition in disordered solids is still being actively investigated.

In this paper, we report the results of molecular dynamics (MD) simulations of a Cu-Zr metallic glass subjected to periodic shear deformation at strain amplitudes near a critical value. We consider a well-annealed sample that was prepared by cooling at a slow rate from the liquid state to room temperature. It will be shown that after a certain number of shear cycles, the glass undergoes a yielding transition characterized by the formation of a system-spanning shear band and a steep increase in the potential energy. We find that when the strain amplitude is reduced towards a critical value, the number of loading cycles until the yielding transition increases as a power-law function, which is in agreement with simulation results for binary LJ glasses well below the glass transition temperature.

The rest of this paper proceeds as follows. In Section 2, we describe the preparation procedure and the deformation protocol. The numerical analysis of the potential energy, shear stress, nonaffine displacements, and atomic configurations is presented in Section 3. A brief summary is given in the last section.

2. MD Simulations

In this study, the $Cu_{50}Zr_{50}$ metallic glass was simulated using the embedded atom method (EAM) potentials [43,44] with the time step $\triangle t = 1.0$ fs. The total number of Cu and Zr atoms is 60,000. The system was initially placed into a periodic box and thoroughly equilibrated at the temperature of 2000 K and zero pressure. Following the cooling protocol described by Fan and Ma [45], the glass former was first cooled to 1500 K at the rate of 10^{13} K/s, then to 1000 K at 10^{12} K/s, and finally to 300 K at 10^{10} K/s. Hence, the effective cooling rate across the glass transition temperature ($T_g \sim 675$ K) was 10^{10} K/s. This preparation procedure was carried out in the NPT ensemble using the Nosé–Hoover thermostat, periodic boundary conditions, and zero external pressure [46].

After cooling to 300 K, the linear size of a cubic domain was fixed to 101.8 Å, and the glass was subjected to periodic shear deformation along the xz plane at constant volume, as follows:

$$\gamma_{xz}(t) = \gamma_0 \sin(2\pi t/T), \quad (1)$$

where $T = 1.0$ ns (10^6 MD time steps) is the oscillation period and γ_0 is the strain amplitude. The MD simulations were performed for strain amplitudes, $0.055 \leqslant \gamma_0 \leqslant 0.064$, near a critical value. The rationale for choosing this range of strain amplitudes is that loading at $\gamma_0 < 0.055$ will not lead to yielding, whereas the yielding transition is reached only after a few cycles when $\gamma_0 > 0.064$. The potential energy, shear stress, and atomic configurations at the end of each cycle were periodically saved for post-processing analysis. Tecplot 360 was used for data visualization [47]. Due to computational constraints, the data were collected only for one realization of disorder.

3. Results

It is generally realized that mechanical properties of bulk metallic glasses strongly depend, among other factors, on preparation history [48,49]. Thus, sufficiently slowly cooled glasses settle at lower energy levels and upon start-up continuous deformation tend to exhibit a pronounced yielding peak characteristic of a brittle response, whereas more

rapidly cooled glasses typically deform in a ductile manner [50]. Moreover, it was recently found that well-annealed binary glasses under periodic loading yield at strain amplitudes smaller than the location of the yielding peak [20,28]. When a critical value is approached from above, the number of cycles to reach the yielding transition increases as a power-law function for binary LJ glasses strained at a temperature well below the glass transition temperature [42]. In the present paper, these results are extended to the case of well-annealed $Cu_{50}Zr_{50}$ metallic glasses at room temperature. We also comment that test runs of more rapidly cooled $Cu_{50}Zr_{50}$ metallic glasses (with the effective cooling rate of 10^{12} K/s) have shown that cyclic loading near the critical strain amplitude induces significant structural relaxation and a rapid decay of the potential energy during a number of transient cycles, which is similar to the results reported for poorly annealed LJ glasses [30].

We first present the dependence of shear stress as a function of loading cycles in Figure 1 for strain amplitudes $\gamma_0 = 0.057$ and 0.064. Note that for the largest strain amplitude $\gamma_0 = 0.064$ considered in the present study, the glass gradually yields after about 40 shear cycles, followed by flow localization upon continued loading. It can be observed that the number of cycles to reach the yielding transition increases significantly at the lower strain amplitude $\gamma_0 = 0.057$. Note that the amplitude of stress oscillations after the yielding transition is nearly the same in both cases, and it is determined by the maximum stress within a narrow region where plastic flow is localized. A similar behavior of the shear stress was observed for low-temperature binary LJ glasses under periodic shear, although the yielding transition in the previous study was associated with a sharp drop in stress during only one shear cycle [42].

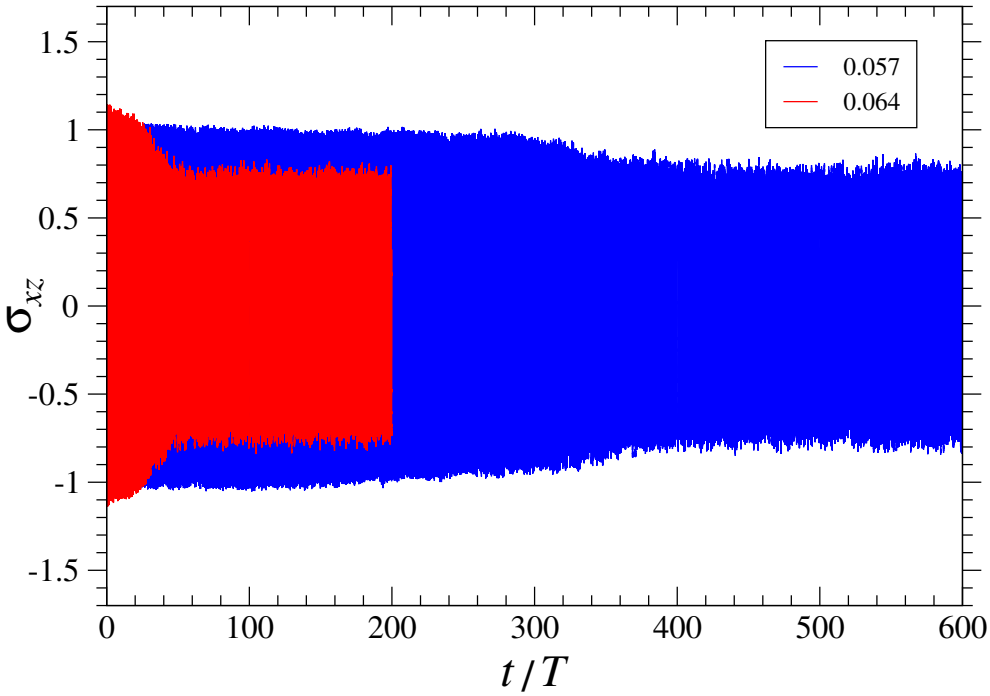

Figure 1. The time dependence of shear stress, σ_{xz} (in units of GPa), for strain amplitudes $\gamma_0 = 0.057$ (blue curve) and $\gamma_0 = 0.064$ (red curve). The period of oscillation is $T = 1.0$ ns.

Next, the variation of the potential energy versus cycle number is displayed in Figure 2 for the same values of the strain amplitude, $\gamma_0 = 0.057$ and 0.064, as in Figure 1. Each of the curves in Figure 2 clearly show three stages of deformation under cyclic loading; namely, a solid-like response, a gradual yielding transition, and localized plastic flow. The relatively large scatter of the data is attributed to thermal fluctuations and finite system size. When loaded at $\gamma_0 = 0.064$, the potential energy at the end of each cycle (the lower envelope) starts to increase abruptly, indicating the occurrence of localized plastic events that eventually lead to the formation of a shear band and the corresponding plateau after

about 60 cycles. By contrast, the initial stage of accumulation of plastic rearrangements at the strain amplitude $\gamma_0 = 0.057$ takes about 300 cycles, and it is followed by a gradual yielding transition during 150 shear cycles.

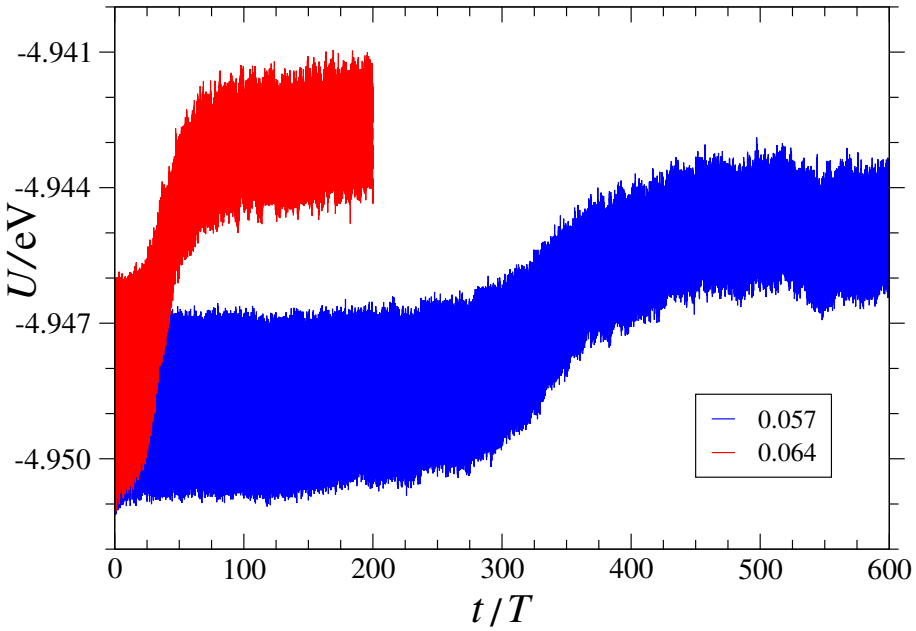

Figure 2. The variation of the potential energy U (in units of eV per atom) as a function of time for strain amplitudes $\gamma_0 = 0.057$ (blue curve) and $\gamma_0 = 0.064$ (red curve). The period of oscillation is $T = 1.0$ ns.

A summary of the data for the potential energy after each cycle (when strain is zero) as a function of the cycle number for strain amplitudes $0.055 \leqslant \gamma_0 \leqslant 0.064$ is presented in Figure 3. It is evident that when the glass is loaded at a lower strain amplitude, the increase in potential energy due to accumulation of plastic events is more gradual and the number of cycles to reach the yielding transition becomes larger. Notice that the system did not yield for at least 700 cycles when periodically deformed at strain amplitudes $\gamma_0 = 0.055$ and 0.056. Therefore, it can be deduced that the critical strain amplitude is between $\gamma_0 = 0.056$ and 0.057. The elastic regime of deformation extends up to 0.056. Further, the results in Figure 3 demonstrate that the well-annealed $Cu_{50}Zr_{50}$ metallic glass can be rejuvenated via cyclic loading at strain amplitudes slightly above a critical value, which is similar to conclusions for binary LJ glasses [42]. For example, the number of cycles needed to increase the potential energy by 0.001 eV per atom varies from about 20 to 300 depending on the strain amplitude (see Figure 3).

It is well known that plastic deformation in metallic glasses involves the so-called nonaffine rearrangements of atoms [51]. In particular, the nonaffine quantity for an atom displaced from $\mathbf{r}_i(t)$ to $\mathbf{r}_i(t + \Delta t)$ can be computed using the matrix $\mathbf{J}_i$, which transforms the positions of neighboring atoms and also minimizes the following function:

$$D^2(t, \Delta t) = \frac{1}{N_i} \sum_{j=1}^{N_i} \left\{ \mathbf{r}_j(t + \Delta t) - \mathbf{r}_i(t + \Delta t) - \mathbf{J}_i \left[\mathbf{r}_j(t) - \mathbf{r}_i(t) \right] \right\}^2, \quad (2)$$

where the sum is taken over N_i atoms that are initially located within 4.0 Å from $\mathbf{r}_i(t)$. Irreversible plastic rearrangements of atoms typically occur when their nonaffine displacements exceed a cage size [16]. It was previously shown that the cage size of $Cu_{50}Zr_{50}$ alloy near the glass transition temperature is about $r_c \approx 0.6$ Å [52].

In Figure 4, we plot the nonaffine quantity, $D^2[(n-1)\,T, T]$, as a function of the number of cycles n for strain amplitudes $0.055 \leqslant \gamma_0 \leqslant 0.064$. The nonaffine quantity,

Equation (2), was evaluated for configurations of atoms at the beginning and end of each cycle when strain is zero and then averaged over all atoms. A close comparison of the data for the potential energy in Figure 3 and the nonaffine measure in Figure 4 reveals a very similar functional dependence of U and D^2 on the cycle number during the yielding transition for each value of γ_0. Notice, for example, that the number of cycles until yielding at $U = -4.948\,\mathrm{eV/atom}$ and $D^2 = 0.5\,\mathrm{\AA}^2$ are essentially the same for strain amplitudes $0.057 \leqslant \gamma_0 \leqslant 0.064$. These results indicate that the potential energy of atomic configurations that evolve via plastic deformation under periodic shear strongly correlates with the average nonaffine displacements of atoms during each cycle.

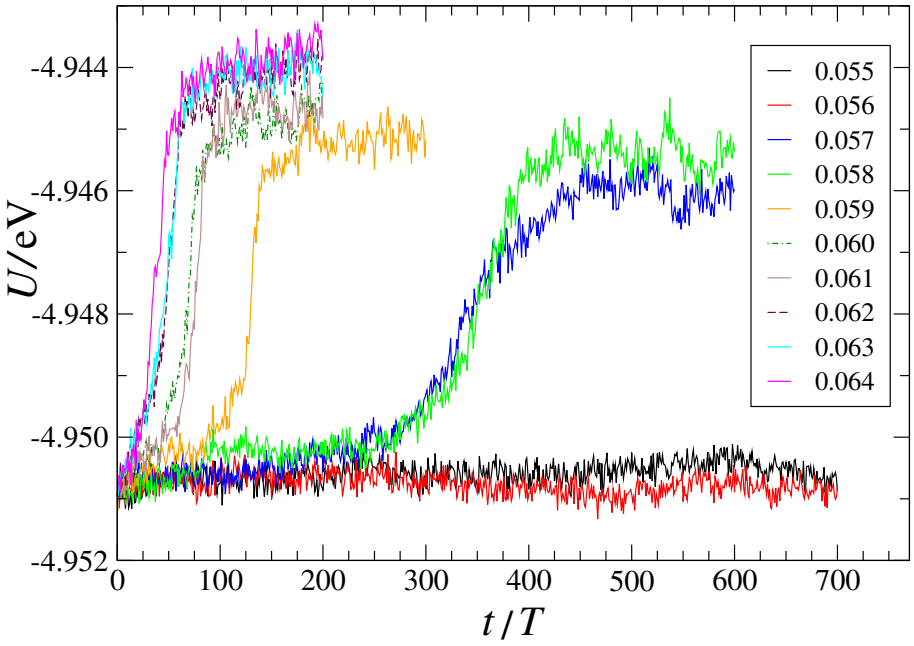

Figure 3. The potential energy at the end of each cycle (when $\gamma_{xz} = 0$) for strain amplitudes in the range $0.055 \leqslant \gamma_0 \leqslant 0.064$. The oscillation period is $T = 1.0\,\mathrm{ns}$.

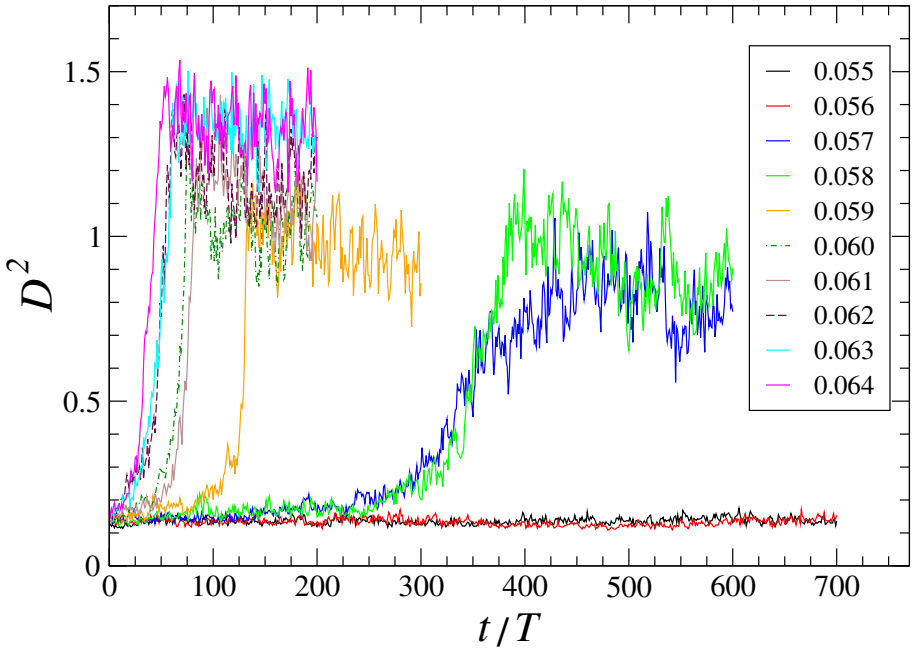

Figure 4. The average of the nonaffine measure, $D^2[(n-1)\,T, T]$ (in units of $\mathrm{\AA}^2$), versus number of cycles for the indicated strain amplitudes. The period of deformation is $T = 1.0\,\mathrm{ns}$.

A more direct way to account for plastic events is to compute a fraction of atoms whose nonaffine displacements during one shear cycle are slightly larger than the typical cage size. The fraction of atoms with relatively large nonaffine displacements, $D^2[(n-1)\,T, T] > 0.49\,\text{Å}^2$, is shown in Figure 5 as a function of the number of cycles for the same values of the strain amplitude as in Figure 4. It can be observed in Figure 5 that the fraction of atoms varies from about 0.02 in the elastic regime at $\gamma_0 = 0.055$ and 0.056 to about 0.45 when a shear band is formed at large strain amplitudes $\gamma_0 = 0.063$ and 0.064. As is evident, the function $n_f(n)$ clearly shows an accumulation of plastic events followed by the yielding transition and extended plastic flow for $\gamma_0 > 0.056$.

The same data for the fraction n_f are replotted in Figure 6 as a function of the ratio n/n_Y, where $n = t/T$ and n_Y is the number of cycles until the yielding transition. Although the data in Figure 6 are somewhat noisy, it can be clearly seen that all curves approximately follow the same trend. In our analysis, the values of n_Y were computed at $n_f = 0.2$ for $\gamma_0 > 0.056$ and reported in the inset to Figure 6. The dependence of the number of cycles until the yielding transition on the strain amplitude can be well captured by the power-law function:

$$n_Y(\gamma_0) = 0.089 \cdot (\gamma_0 - \gamma_c)^{-1.25}, \tag{3}$$

where the critical value of strain amplitude is taken $\gamma_c = 0.056$. The best fit to the data yields an exponent of -1.25 in Equation (3), implying a possible divergence of n_Y upon approaching γ_c from above. In practice, the power-law function, Equation (3), can be used not only to determine the number of cycles until failure at a given strain amplitude but also to estimate a number cycles needed to rejuvenate the glass by inducing small-scale plastic events. For example, when the glass is loaded for $n = n_Y/2$ cycles, then the fraction of plastic displacements becomes $n_f \approx 0.05$ for $\gamma_0 > 0.056$ (see Figure 6).

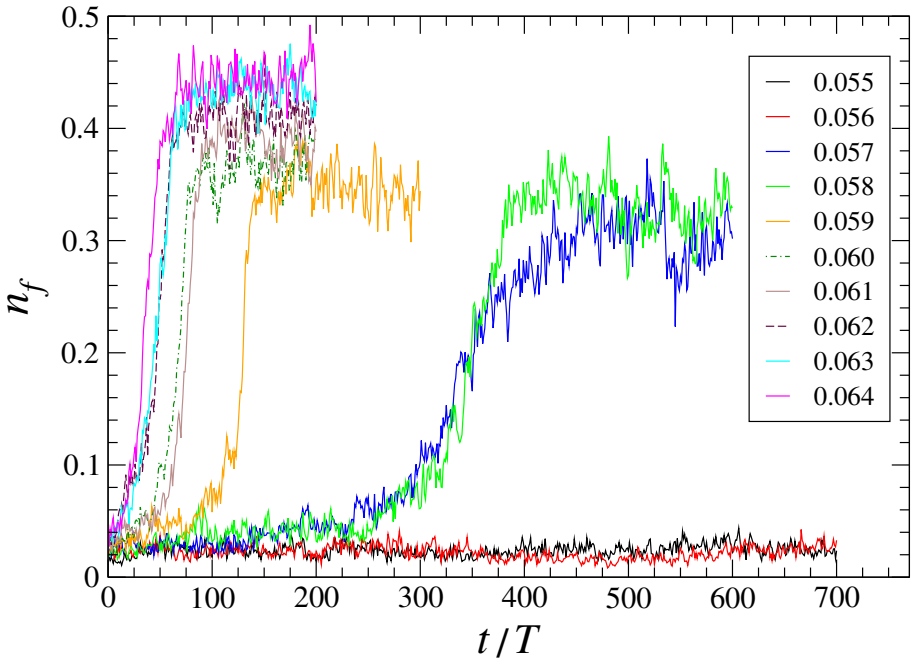

Figure 5. The fraction of atoms with large nonaffine displacements during one loading cycle, $D^2[(n-1)\,T, T] > 0.49\,\text{Å}^2$, as a function of the number of cycles, $n = t/T$, for the indicated strain amplitudes γ_0. The oscillation period is $T = 1.0$ ns.

Note that a power-law dependence with a different exponent of -1.66 was reported for periodically sheared binary LJ glasses at a temperature well below T_g [42]. It should be commented that the power-law function, $n_Y(\gamma_0)$ describes the data for LJ and Cu-Zr glasses that were both prepared by cooling across the glass transition at a 'computationally' slow rate. However, it was found that the critical strain amplitude at zero temperature

increases when a glass is relocated into deeper regions of its energy landscape by using either the swap Monte Carlo algorithm [29] or mechanical annealing [34]. A recent study showed an example of how the yielding transition becomes increasingly delayed in more stable (mechanically annealed) glasses at low temperatures when cyclic loading is applied at a fixed strain amplitude [33]. Moreover, MD simulations of periodically loaded LJ glasses at about half T_g revealed that although the yielding transition is delayed in better annealed glasses, the critical strain amplitude remains unchanged [40]. Therefore, it is still unclear how, in general, the critical strain amplitude and the power-law dependence, $n_Y(\gamma_0)$, are affected by the degree of annealing for cyclically loaded glasses at a finite temperature.

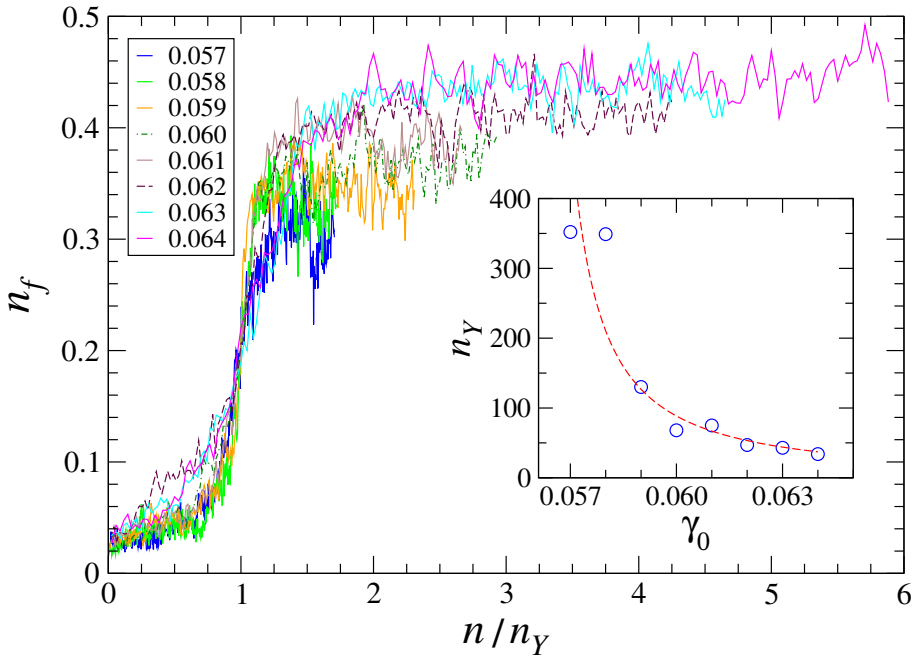

Figure 6. The fraction of atoms with large nonaffine displacements during one cycle, $D^2[(n-1)\,T, T] > 0.49$ Å^2, versus n/n_Y, where $n = t/T$ and n_Y is the number of cycles until yielding. The inset shows n_Y as a function of γ_0. The dashed line is the best fit to the data given by Equation (3).

The spatial extent of plastic events in the metallic glass under cyclic shear is illustrated in Figure 7 for the strain amplitude $\gamma_0 = 0.064$ and in Figure 8 for $\gamma_0 = 0.057$. For clarity, only atoms with relatively large nonaffine displacements during one cycle, $D^2[(n-1)\,T, T] > 0.49$ Å^2, are shown when strain is zero. It can be seen in Figure 7a that during the fourth cycle at the strain amplitude $\gamma_0 = 0.064$, atoms with large nonaffine displacements form several isolated clusters. Upon further loading, the steep increase in U (see Figure 2) and n_f (see Figure 5) is characterized by the formation of an extended cluster of atoms that percolates across the entire system, as shown in Figure 7b,c. After 80 cycles, the shear band develops along the xy plane, shown in Figure 7d, which is consistent with the plateau level in the potential energy reported in Figure 2. A similar trend can be observed in Figure 8 for the strain amplitude $\gamma_0 = 0.057$, except that the yielding transition is delayed by about 300 cycles and the shear band is formed along the perpendicular plane yz. The results in Figure 8a also confirm that after about $n_Y/2$ cycles at $\gamma_0 = 0.057$, plastic deformation involves only small-scale clusters ($n_f \approx 0.04$).

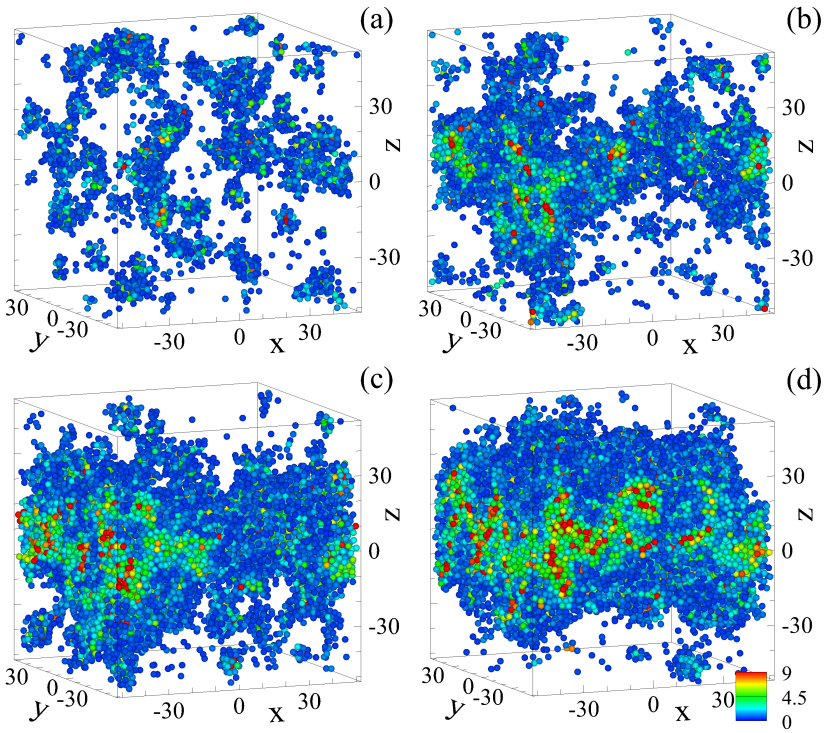

Figure 7. The atomic configurations of the metallic glass periodically loaded at the strain amplitude $\gamma_0 = 0.064$. The nonaffine displacements are only shown for atoms with the nonaffine measure (**a**) $D^2(3\,T, T) > 0.49\,\text{Å}^2$, (**b**) $D^2(30\,T, T) > 0.49\,\text{Å}^2$, (**c**) $D^2(40\,T, T) > 0.49\,\text{Å}^2$, and (**d**) $D^2(80\,T, T) > 0.49\,\text{Å}^2$. The magnitude of D^2 is indicated by the legend color. The Zr and Cu atoms are not depicted to scale.

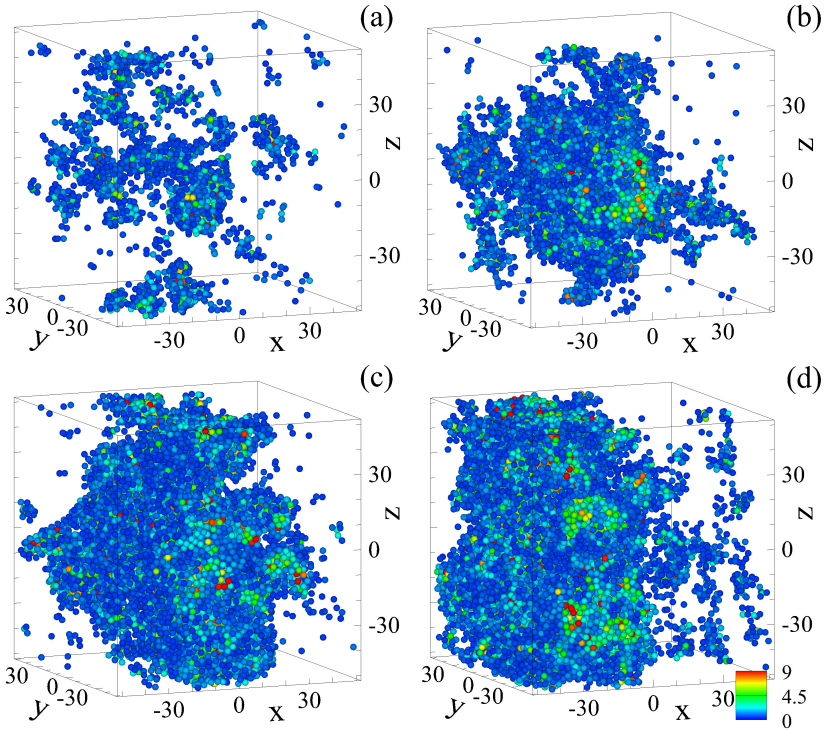

Figure 8. Selected configurations of atoms in the binary glass deformed with the strain amplitude $\gamma_0 = 0.057$. The nonaffine measure is (**a**) $D^2(150\,T, T) > 0.49\,\text{Å}^2$, (**b**) $D^2(320\,T, T) > 0.49\,\text{Å}^2$, (**c**) $D^2(380\,T, T) > 0.49\,\text{Å}^2$, and (**d**) $D^2(500\,T, T) > 0.49\,\text{Å}^2$. The magnitude of D^2 is indicated according to the legend in the panel (**d**).

4. Conclusions

In summary, we studied the effect of periodic shear deformation on the yielding transition in metallic glasses using molecular dynamics simulations. We considered a $Cu_{50}Zr_{50}$ metallic glass prepared by slow cooling from the melt to room temperature and then subjected to periodic shear at constant volume. It was shown that during loading for hundreds of cycles at strain amplitudes slightly below a critical value, the potential energy at the end of each cycle remains nearly unchanged and plastic deformation proceeds via localized clusters of atoms with relatively large nonaffine displacements. When loaded at larger strain amplitudes, the glass becomes gradually rejuvenated via collective irreversible displacements of atoms from cycle to cycle until the yielding transition and the formation of a system-spanning shear band. Remarkably, the number of cycles to reach the yielding transition approximately follows a power-law dependence on the difference between the strain amplitude and the critical value. Despite a different value of the power-law exponent, these conclusions are in agreement with the results for binary Lennard-Jones glasses periodically deformed at a temperature well below the glass transition temperature.

Funding: The financial support from the National Science Foundation (grant CNS-1531923) is gratefully acknowledged. Molecular dynamics simulations and the post-processing analysis were performed at the Wright State University's Computing Facility and the Ohio Supercomputer Center using the LAMMPS code [46].

Data Availability Statement: The data presented in this study are available upon request.

Acknowledgments: Molecular dynamics simulations and the post-processing analysis were performed at the Wright State University's Computing Facility and the Ohio Supercomputer Center using the LAMMPS code [46].

Conflicts of Interest: The author declares that he has no conflict of interest.

References

1. Kruzic, J.J. Bulk metallic glasses as structural materials: A review. *Adv. Eng. Mater.* **2016**, *18*, 1308. [CrossRef]
2. Qiao, J.C.; Wang, Q.; Pelletier, J.M.; Kato, H.; Casalini, R.; Crespo, D.; Pineda, E.; Yao, Y.; Yang, Y. Structural heterogeneities and mechanical behavior of amorphous alloys. *Prog. Mater. Sci.* **2019**, *104*, 250. [CrossRef]
3. Jia, H.; Wang, G.; Chen, S.; Gao, Y.; Li, W.; Liaw, P.K. Fatigue and fracture behavior of bulk metallic glasses and their composites. *Prog. Mater. Sci.* **2018**, *98*, 168. [CrossRef]
4. Menzel, B.C.; Dauskardt, R.H. Stress-life fatigue behavior of a Zr-based bulk metallic glass. *Acta Mater.* **2006**, *54*, 935. [CrossRef]
5. Sha, Z.; Lin, W.; Poh, L.H.; Xing, G.; Liu, Z.; Wang, T.; Gao, H. Fatigue of metallic glasses. *Appl. Mech. Rev.* **2020**, *72*, 050801. [CrossRef]
6. Spaepen, F. A microscopic mechanism for steady state inhomogeneous flow in metallic glasses. *Acta Metall.* **1977**, *25*, 407. [CrossRef]
7. Argon, A.S. Plastic deformation in metallic glasses. *Acta Metall.* **1979**, *27*, 47. [CrossRef]
8. Parley, J.T.; Sastry, S.; Sollich, P. Mean-field theory of yielding under oscillatory shear. *Phys. Rev. Lett.* **2022**, *128*, 198001. [CrossRef]
9. Cochran, J.O.; Callaghan, G.L.; Fielding, S.M. Slow fatigue and highly delayed yielding via shear banding in oscillatory shear. *arxiv* **2022**, arXiv:2211.11677
10. Priezjev, N.V. Heterogeneous relaxation dynamics in amorphous materials under cyclic loading. *Phys. Rev. E* **2013**, *87*, 052302. [CrossRef]
11. Regev, I.; Lookman, T.; Reichhardt, C. Onset of irreversibility and chaos in amorphous solids under periodic shear. *Phys. Rev. E* **2013**, *88*, 062401. [CrossRef] [PubMed]
12. Fiocco, D.; Foffi, G.; Sastry, S. Oscillatory athermal quasistatic deformation of a model glass. *Phys. Rev. E* **2013**, *88*, 020301(R). [CrossRef]
13. Regev, I.; Weber, J.; Reichhardt, C.; Dahmen, K.A.; Lookman, T. Reversibility and criticality in amorphous solids. *Nat. Commun.* **2015**, *6*, 8805. [CrossRef] [PubMed]
14. Luo, J.; Dahmen, K.; Liaw, P.K.; Shi, Y. Low-cycle fatigue of metallic glass nanowires. *Acta Mater.* **2015**, *87*, 225. [CrossRef]
15. Sha, Z.D.; Qu, S.X.; Liu, Z.S.; Wang, T.J.; Gao, H. Cyclic deformation in metallic glasses. *Nano Lett.* **2015**, *15*, 7010. [CrossRef] [PubMed]
16. Priezjev, N.V. Reversible plastic events during oscillatory deformation of amorphous solids. *Phys. Rev. E* **2016**, *93*, 013001. [CrossRef]
17. Kawasaki, T.; Berthier, L. Macroscopic yielding in jammed solids is accompanied by a non-equilibrium first-order transition in particle trajectories. *Phys. Rev. E* **2016**, *94*, 022615. [CrossRef]

18. Priezjev, N.V. Nonaffine rearrangements of atoms in deformed and quiescent binary glasses. *Phys. Rev. E* **2016**, *94*, 023004. [CrossRef] [PubMed]
19. Ranganathan, R.; Shi, Y.; Keblinski, P. Commonalities in frequency-dependent viscoelastic damping in glasses in the MHz to THz regime. *J. Appl. Phys.* **2017**, *122*, 145103. [CrossRef]
20. Leishangthem, P.; Parmar, A.D.S.; Sastry, S. The yielding transition in amorphous solids under oscillatory shear deformation. *Nat. Commun.* **2017**, *8*, 14653. [CrossRef]
21. Priezjev, N.V. Collective nonaffine displacements in amorphous materials during large-amplitude oscillatory shear. *Phys. Rev. E* **2017**, *95*, 023002. [CrossRef]
22. Priezjev, N.V. Molecular dynamics simulations of the mechanical annealing process in metallic glasses: Effects of strain amplitude and temperature. *J. Non-Cryst. Solids* **2018**, *479*, 42. [CrossRef]
23. Priezjev, N.V. The yielding transition in periodically sheared binary glasses at finite temperature. *Comput. Mater. Sci.* **2018**, *150*, 162. [CrossRef]
24. Parmar, A.D.S.; Kumar, S.; Sastry, S. Strain localization above the yielding point in cyclically deformed glasses. *Phys. Rev. X* **2019**, *9*, 021018. [CrossRef]
25. Priezjev, N.V. Slow relaxation dynamics in binary glasses during stress-controlled, tension-compression cyclic loading. *Comput. Mater. Sci.* **2018**, *153*, 235. [CrossRef]
26. Bai, Y.; She, C. Atomic structure evolution in metallic glasses under cyclic deformation. *Comput. Mater. Sci.* **2019**, *169*, 109094. [CrossRef]
27. Priezjev, N.V. Accelerated relaxation in disordered solids under cyclic loading with alternating shear orientation. *J. Non-Cryst. Solids* **2019**, *525*, 119683. [CrossRef]
28. Priezjev, N.V. Shear band formation in amorphous materials under oscillatory shear deformation. *Metals* **2020**, *10*, 300. [CrossRef]
29. Yeh, W.T.; Ozawa, M.; Miyazaki, K.; Kawasaki, T.; Berthier, L. Glass stability changes the nature of yielding under oscillatory shear. *Phys. Rev. Lett.* **2020**, *124*, 225502. [CrossRef]
30. Priezjev, N.V. Alternating shear orientation during cyclic loading facilitates yielding in amorphous materials. *J. Mater. Eng. Perform.* **2020**, *29*, 7328. [CrossRef]
31. Tang, L.; Ma, G.; Liu, H.; Zhou, W.; Bauchy, M. Bulk metallic glasses' response to oscillatory stress is governed by the topography of the energy landscape. *J. Phys. Chem. B* **2020**, *124*, 11294. [CrossRef] [PubMed]
32. Wang, P.; Yang, X. Atomistic investigation of aging and rejuvenation in CuZr metallic glass under cyclic loading. *Comput. Mater. Sci.* **2020**, *185*, 109965. [CrossRef]
33. Priezjev, N.V. A delayed yielding transition in mechanically annealed binary glasses at finite temperature. *J. Non-Cryst. Solids* **2020**, *548*, 120324. [CrossRef]
34. Bhaumik, H.; Foffi, G.; Sastry, S. The role of annealing in determining the yielding behavior of glasses under cyclic shear deformation. *PNAS* **2021**, *118*, 2100227118. [CrossRef]
35. Priezjev, N.V. Accessing a broader range of energy states in metallic glasses by variable-amplitude oscillatory shear. *J. Non-Cryst. Solids* **2021**, *560*, 120746. [CrossRef]
36. Yang, Y.; Li, H.; Yang, Z.; Liu, J.; Kateye, E.K.; Zhao, J. Notch fatigue of $Cu_{50}Zr_{50}$ metallic glasses under cyclic loading: Molecular dynamics simulations. *Commun. Theor. Phys.* **2021**, *73*, 065501. [CrossRef]
37. Priezjev, N.V. Yielding transition in stable glasses periodically deformed at finite temperature. *Comput. Mater. Sci.* **2021**, *200*, 110831. [CrossRef]
38. Cui, S.; Liu, H.; Peng, H. Anisotropic correlations of plasticity on the yielding of metallic glasses. *Phys. Rev. E* **2022**, *106*, 014607. [CrossRef]
39. Zhao, L.; Ouyang, D.; Wang, Y.; Chan, K. Improving fatigue performance of metallic glasses with crystalline metal coating revealed by atomistic simulations. *J. Non-Cryst. Solids* **2022**, *586*, 121559. [CrossRef]
40. Priezjev, N.V. Mechanical annealing and yielding transition in cyclically sheared binary glasses. *J. Non-Cryst. Solids* **2022**, *590*, 121697. [CrossRef]
41. Shang, B.; Jakse, N.; Guan, P.; Wang, W.; Barrat, J.-L. Influence of oscillatory shear on nucleation in metallic glasses: A molecular dynamics study. *Acta Mater.* **2023**, *246*, 118668. [CrossRef]
42. Priezjev, N.V. Fatigue failure of amorphous alloys under cyclic shear deformation. *Comput. Mater. Sci.* **2023**, *226*, 112230. [CrossRef]
43. Cheng, Y.Q.; Ma, E.; Sheng, H.W. Atomic level structure in multicomponent bulk metallic glass. *Phys. Rev. Lett.* **2009**, *102*, 245501. [CrossRef]
44. Cheng, Y.Q.; Ma, E. Atomic-level structure and structure-property relationship in metallic glasses. *Prog. Mater. Sci.* **2011**, *56*, 379. [CrossRef]
45. Fan, Z.; Ma, E. Predicting orientation-dependent plastic susceptibility from static structure in amorphous solids via deep learning. *Nat. Commun.* **2021**, *12*, 1506. [CrossRef]
46. Plimpton, S.J. Fast parallel algorithms for short-range molecular dynamics. *J. Comp. Phys.* **1995**, *117*, 1. [CrossRef]
47. Tecplot 360 Version 2015r2. 2015. Available online: https://www.tecplot.com/products/tecplot-360/ (accessed on 16 September 2023).
48. Egami, T.; Iwashita, T.; Dmowski, W. Mechanical properties of metallic glasses. *Metals* **2013**, *3*, 77. [CrossRef]

49. Sun, Y.; Concustell, A.; Greer, A.L. Thermomechanical processing of metallic glasses: Extending the range of the glassy state. *Nat. Rev. Mater.* **2016**, *1*, 16039. [CrossRef]
50. Hufnagel, T.C.; Schuh, C.A.; Falk, M.L. Deformation of metallic glasses: Recent developments in theory, simulations, and experiments. *Acta Mater.* **2016**, *109*, 375. [CrossRef]
51. Falk, M.L.; Langer, J.S. Dynamics of viscoplastic deformation in amorphous solids. *Phys. Rev. E* **1998**, *57*, 7192. [CrossRef]
52. Wang, X.; Xu, W.-S.; Zhang, H.; Douglas, J.F. Universal nature of dynamic heterogeneity in glass-forming liquids: A comparative study of metallic and polymeric glass-forming liquids. *J. Chem. Phys.* **2019**, *151*, 184503. [CrossRef] [PubMed]